Supporting Information Figure S1–S9

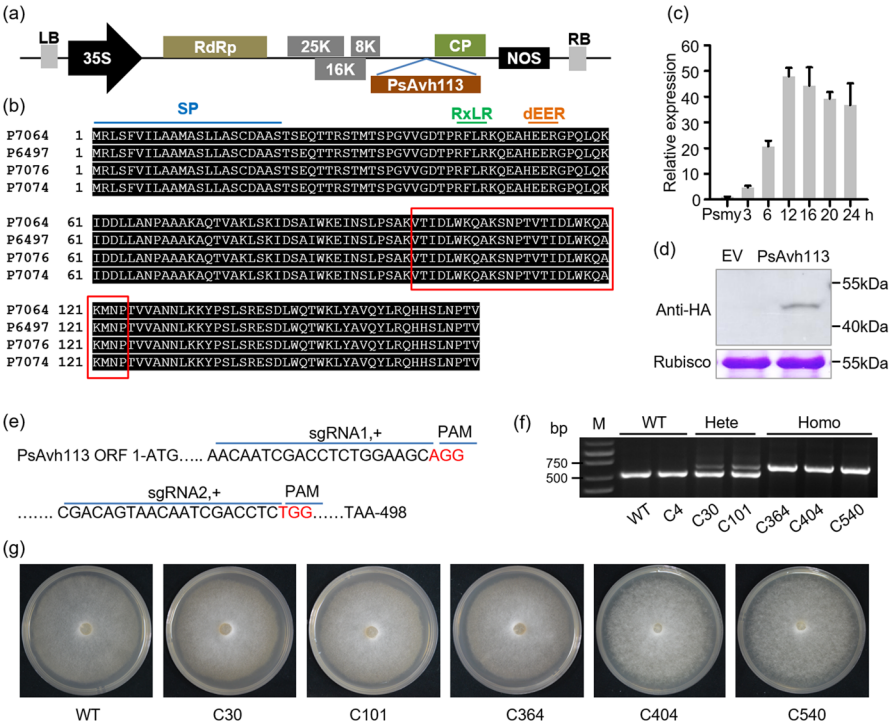

Figure S1 PVX-based recombinant construct and expression pattern of *PsAvh113*.

(**a**) Schematic representation of the recombinant PVX-*PsAvh113* construct. (**b**) The amino acids of PsAvh113 is conserved in four sequenced *P. sojae*. SP, signal peptide, the sequence of RxLR and dEER motif is indicated. Red square represents sequences of two IR motifs. (**c**) Transcript levels of *PsAvh113* at different infection stage of *P. sojae* in Huachun6 roots. Total RNA was extracted from mycelia (MY) or infected soybean roots at 3, 6, 12, 24 and 48 h post inoculation (hpi). The *P. sojae* Actin gene (VMD GeneID: 108986) was used as an internal control. (**d**) Western blotting showing the expression of PsAvh113 in soybean hairy roots. (**e**) The sequences of two unique sgRNAs were designed to knockout the *PsAvh113* gene from the *P. sojae* wild-type P6497 using the CRISPR/Cas9 system. These sgRNAs were located the coding regions of PsAvh113. (**f**) Analysis of *P. sojae* transformants. The homozygous transformants were determined by performing PCR on genomic DNA samples, which came from the wildtype (WT), empty-vector control line (EV), and *PsAvh113*-knockout mutants (C30, C101, C364, C404, C540). WT, wild-type strain; Hete, Heterozygous transformants; Homo, Homozygous transformants. (**g**) Colony morphology and vegetative growth of wild-type P6497 and PsAvh113 transformants on 10% V8 juice agar media (V8) with G418 antibiotics. Photographs were taken after 7-day incubation in the dark at 25°C.

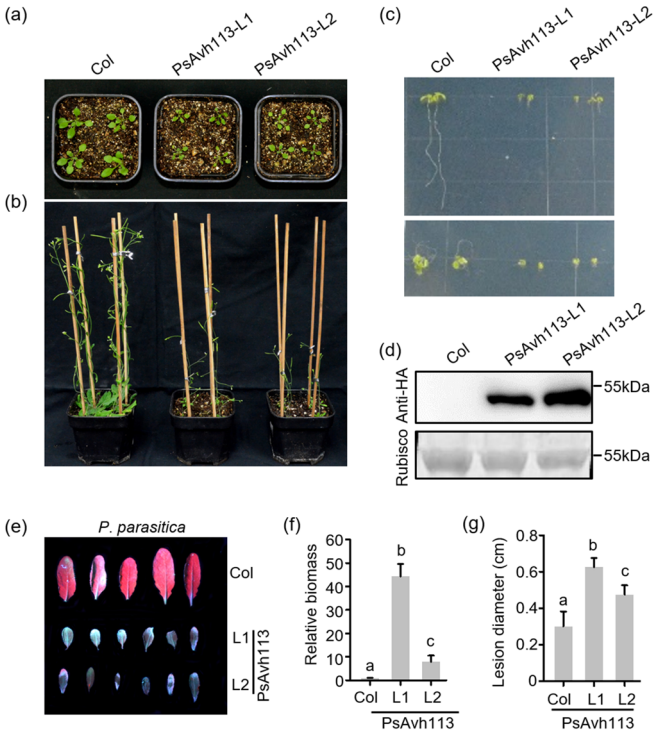

Figure S2 Overexpression of *PsAvh113* affects plant development and defense response in *Arabidopsis*.

(**a-c**) Phenotype of wild type and the transgenic *Arabidopsis* lines expressing PsAvh113, which exhibited moderate retarded development and minor late flowering compared with the wild-type plants. 21-day old transgenic plant (**a**). The transgenic plants (right) were shorter than wild type (left) after 42 days (**b**). 10-day-old plants in MS medium (**c**). (**d**) Western blotting showing expression of PsAvh113 in transgenic *Arabidopsis* plants. (**e**) Disease symptoms in Col and transgenic *Arabidopsis* lines of PsAvh113 upon *P. parasitica* infection. 3-4-week-old leaves were detached and inoculated with zoospore suspensions of *P. parasitica*. Disease was monitored and images were taken at 2 dpi. (**f**) qRT-PCR analysis of relative *Phytophthora* biomass following *P. parasitica* infection. Fifteen infected leaves were counted at 48 hpi. (g) Sizes of lesions caused by *P. parasitica* infection on leaves overexpressing *PsAvh113*. *PpUBC2* and *AtActin* genes were used as internal controls. Data in (**f**) and (**g**) represent mean ± standard error (SE). Different letters indicate statistically significant differences ($P < 0.01$; Duncan's multiple range test). The experiment was performed in triplicate with similar results.

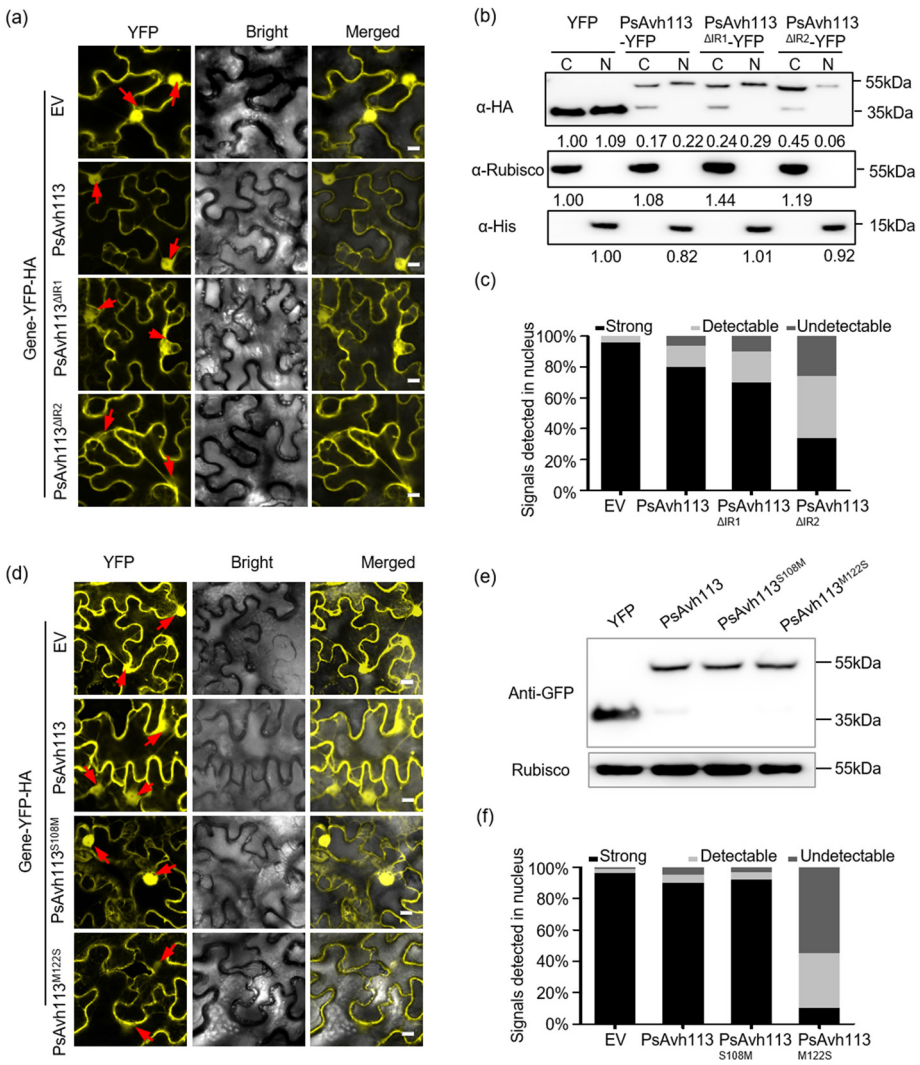

Figure S3 Analysis of PsAvh113 and its mutated derivatives by subcellular localization, the cytoplasm and the nucleus protein separation.

(**a**) Subcellular localizations of PsAvh113-YFP and YFP-tagged PsAvh113 mutants in *N. benthamiana* leaves based on *A. tumefaciens*-mediated transient expression. Fluorescence was detected in epidermal cells of infiltrated tissues by confocal microscopy at 48 h post inoculation (hpi). Red arrowheads point to the tips of nucleus. Bars, 40 μm. (b) Western blot analysis of PsAvh113-YFP-HA or PsAvh113 mutants-YFP-HA in cytoplasmic and nuclear extracts from *N. benthamiana* leaves with anti-HA antibody, and YFP-HA was used as control. Rubisco and histone H3 were detected as fractionation markers for the cytoplasm and the nucleus, respectively. (c) A total of 50 epidermal cells of *N. benthamiana* expressing YFP-HA, PsAvh113-YFP-HA or PsAvh113 mutants-YFP-HA, respectively, were screened for the distribution of fluorescence. (d) Subcellular localizations of PsAvh113-YFP, YFP-tagged PsAvh113^{S108M} and PsAvh113^{M122S} in *N. benthamiana* leaves. Fluorescence was detected at 48 h post inoculation (hpi). Red arrowheads point to the tips of nucleus. Bars, 40 μm. (e) Western

blot analysis of PsAvh113-, PsAvh113^{S108M}- and PsAvh113^{M122S}-YFP-HA with anti-GFP antibody. Rubisco was used as control. (f) A total of 50 epidermal cells of *N. benthamiana* expressing YFP-HA, PsAvh113-, PsAvh113^{S108M}- and PsAvh113^{M122S} -YFP-HA, respectively, were screened for the distribution of fluorescence. In (c) and (f), the Strong means strong signal in nucleus, the detectable means partial signal in nucleus and the undetectable means no signal in nucleus.

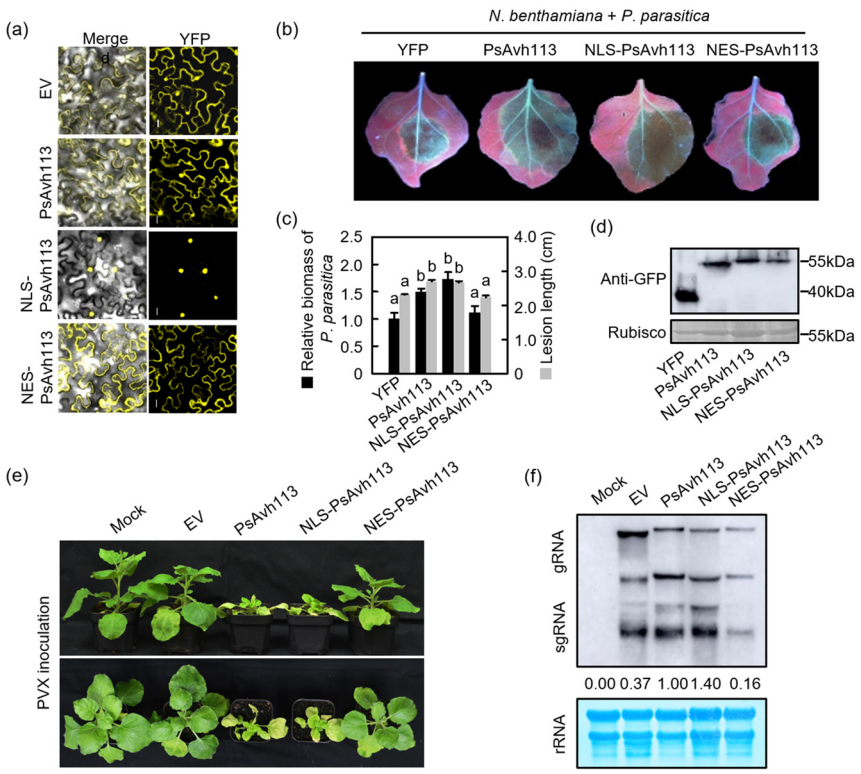

Figure S4 The nuclear localization of PsAvh113 is required for its virulence activity in plants.

(**a**) Subcellular localizations of PsAvh113-YFP, NLS-PsAvh113-YFP and NES-PsAvh113-YFP in *N. benthamiana* leaves based on *A.* tumefaciens-mediated transient expression. A nuclear export sequence (NES), or a nuclear localization sequence (NLS) into the N terminus of PsAvh113, respectively. Fluorescence was detected in epidermal cells of infiltrated tissues by confocal microscopy at 48 hpi. Bars, 40 μm. (**b**) Disease symptoms on the *N. benthamiana* leaves expressing *Agrobacterium* harboring *EV*, *PsAvh113*, *NLS-PsAvh113* or *NES-PsAvh113* construct, respectively. Then the detached leaves were inoculated with zoospore suspensions of *P. parasitica*. Disease symptoms were monitored and leaves were photographed at 2 d post inoculation (dpi). (**c**) Measurements of relative biomass and oospore count on susceptible soybean HC6. Sizes of lesions in infected leaves is shown in gray. Quantification of the relative *P. parasitica* biomass is shown in dark. Fifteen infected leaves were counted at 48 hpi. *PpUBC2* and *NbEF1a* genes were used as internal controls. (d) Western blotting showing expression of the recombinant proteins in *N. benthamiana*. (**e**) Expression of *PsAvh113* or *NLS-PsAvh113* promote virus symptoms to hinder plant growth and development in *N. benthamiana*. Photos were taken at 21 dpi. (f) RNA blotting showing the accumulation of PVX genomic and subgenomic RNA at 14 d post-infection. Non-infected plants (mock) were used as a negative control. Data in (**c**) represent mean ± standard error (SE). Different letters indicate statistically

significant differences ($P < 0.01$; Duncan's multiple range test). The experiment was performed in triplicate with similar results.

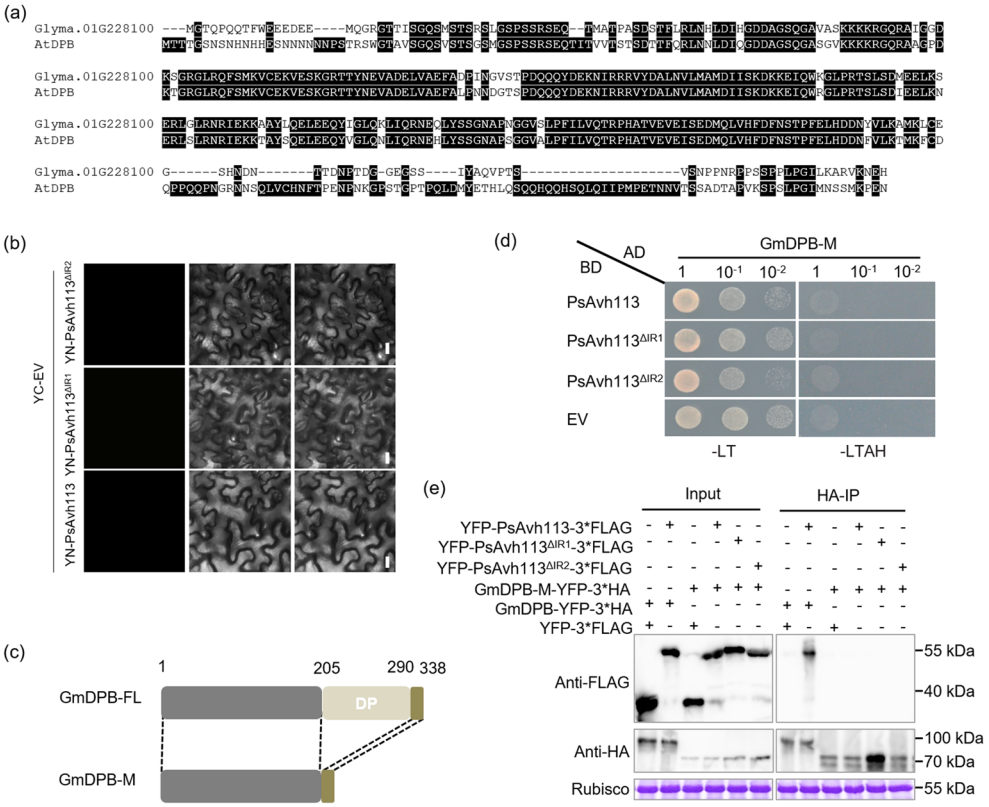

Figure S5 Analysis of interaction between PsAvh113 and GmDPB *in vitro* and *in vivo*.

(**a**) Amino acid sequence alignment of DPB from *Arabidopsis* and soybean (Glyma.01G228100). Identical residues are shaded black. (**b**) BiFC assays displaying that YN-PsAvh113, YN-PsAvh113 $^{\triangle IR1}$ or YN-PsAvh113 $^{\triangle IR2}$ did not interact with YC-EV. DP, Dimerization domain of DP. (**c**) Schematic diagram showing the protein structures of GmDPB and its deletion mutants. (**d**) Y2H assay showing that the key domain of GmDPB mediates its interaction with PsAvh113. (**e**) Co-immunoprecipitation assays showing that PsAvh113 interacts with GmDPB, but not GmDPB mutants. Total proteins were extracted from *N. benthamiana* leaves expressing *GmDPB-HA* or HA-tagged *GmDPB* deletion mutant or and *PsAvh113-FLAG* or Flag-tagged *PsAvh113* mutants. Immune complexes were pulled down using anti-HA agarose gel.

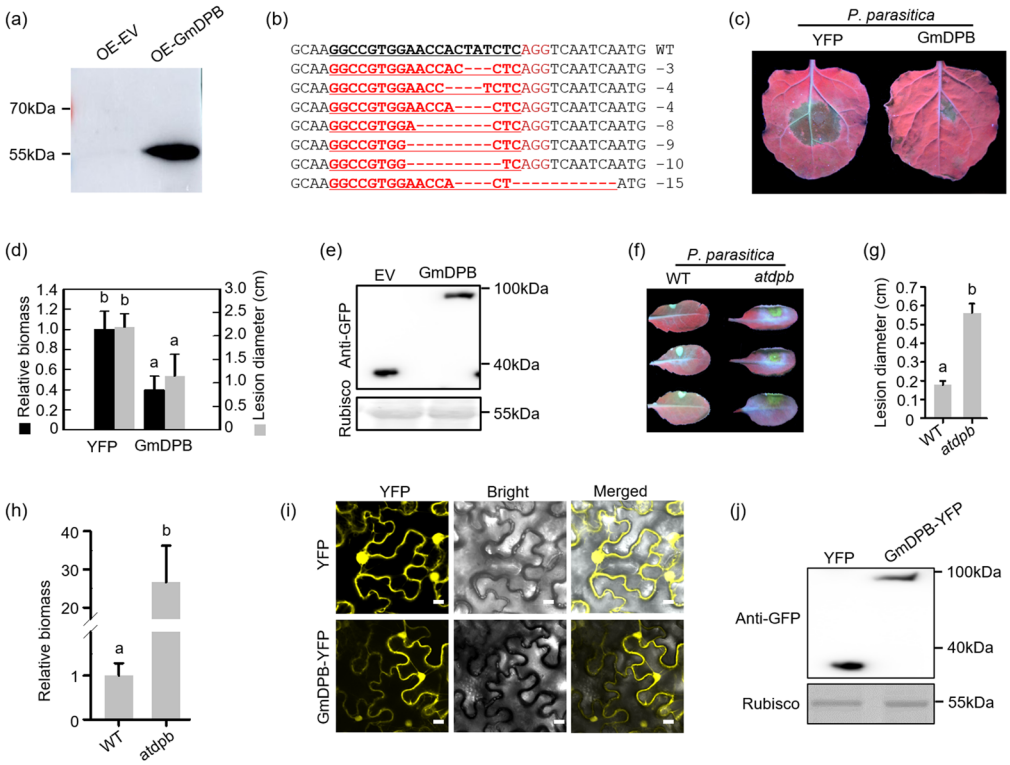

Figure S6 DPB genes in soybean and *Arabidopsis* positively regulate plant immunity against *Phytophthora* infection.

(**a**) Western blot confirming expression of *GmDPB* in *GmDPB*-overexpressed hairy roots. (**b**) Sanger sequencing in wild type soybean HC6 and *GmDPB*-edited hairy roots. (**c**) Overexpression of *GmDPB* decreases susceptibility to *P. parasitica* in *N. benthamiana*. Leaves were detached and inoculated with zoospore suspensions of *P. parasitica* after 24h post-infiltration. Disease symptoms were monitored and photographs were taken at 2 dpi. (**d**) Statistics analysis and relative biomass quantification of (**c**). Lesion size caused by *P. parasitica* infection is illustrated in gray. Relative biomass quantification data is shown in dark. *PpUBC2* and *NbEF1a* genes were used as internal controls. (**e**) Western blot confirming expression of GmDPB in *N. benthamiana* leaves. (**f**) The *atdpb* muant increase the susceptibility to *P. parasitica* in *Arabidopsis*. Disease symptoms were monitored and leaves were photographed at 2 d post inoculation (dpi). (**g**) Sizes of lesions caused by *P. parasitica* infection on *atdpb* mutant leaves. Fifteen infected leaves were counted at 48 hpi. (**h**) qRT-PCR analysis of relative *Phytophthora* biomass followed by *P. parasitica* infection. *PpUBC2* and *AtActin* genes were used as internal controls. (**i**) Subcellular localizations of YFP-tagged GmDPB in *N. benthamiana* leaves based on *A. tumefaciens*-mediated transient expression**,** showing that GmDPB-YFP was localized in the nucleus and cytoplasm. Fluorescence was detected in epidermal cells of infiltrated tissues by confocal microscopy at 48 hpi. Bars, 40 μm. (**j**) Western blot confirming expression of GmDPB in *N. benthamiana* leaves. Data in (**d**), (**g**) and (**h**)

represent mean ± standard error (SE). Different letters indicate statistically significant differences ($P < 0.01$; Duncan's multiple range test). The experiment was performed in triplicate with similar results.

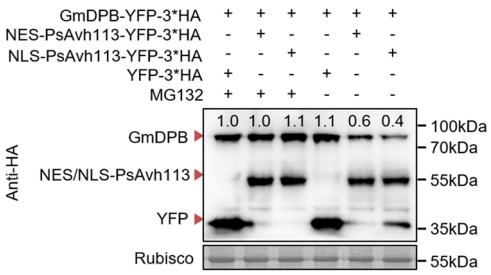

Figure S7 PsAvh113 affects the stability of GmDPB protein in cytoplasm and nucleus. Western blot showing that co-infiltration of GmDPB with NES-PsAvh113 and NLS-PsAvh113 reduce GmDPB abundance in *N. benthamiana* and the degradation of GmDPB protein was blocked by application of proteasome inhibitor MG132 in *N. benthamiana*.

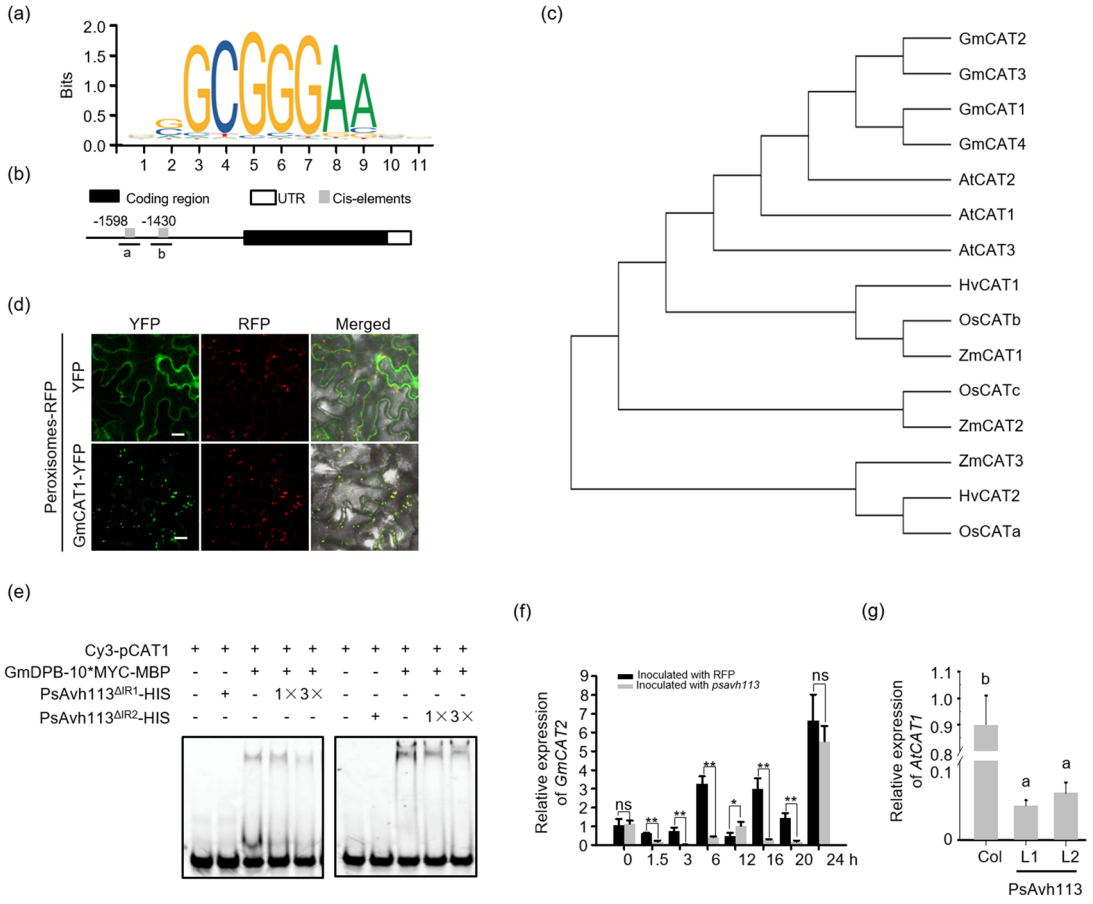

Figure S8 Analysis of subcellular localization and expression of *GmCAT1*.

(**a**) Sequence logo of the overrepresented motif enrich in the set of human *DPB* target genes. The overall height of each stack indicates the sequence conservation at that position (measured in bits), whereas the height of symbols within the stack reflects the relative frequency of the corresponding nucleic acid at that position. (**b**) Two cis-elements in the ~1.5 kb region upstream of the *GmCAT1* promoter. (**c**) Phylogeny of GmCAT orthologs. The phylogenetic tree was constructed by the Neighbor-Joining (NJ) approach. *Glycine max* (GmCAT1, Glyma.14G223500; GmCAT2, Glyma.04G017500; GmCAT3, Glyma.06G017900; GmCAT4, Glyma.17G261700); *Oryza sativa* (OsCATa, Os02g0115700; OsCATb, Os06g0727200; OsCATc, Os03g0131200); *Zea mays* (ZmCAT1, X12538; ZmCAT1, X54819; ZmCAT3, X12539); *Hordeum vulgate* (HvCAT1,U20777; HvCAT2,U20778); *Arabidopsis thaliana* (AtCAT1, AT1G20630; AtCAT2, AT4G35090; AtCAT3, AT1G20620). (**d**) Subcellular localizations of GmCAT1-YFP and peroxisomes-RFP in *N. benthamiana* leaves based on *A. tumefaciens*-mediated transient expression. Fluorescence was detected in epidermal cells of infiltrated leaves by confocal microscopy at 48 hpi. Bars, 40 μm. (**e**) EMSA experiments showed that the binding degree of *pGmCAT1* promoter to GmDPB was affected by PsAvh113 $^{\triangle IR1}$, and the effect was positively correlated with its concentration. (**f**) The Graph showing the

relative expression levels of *GmCAT2*. Leaves were sampled at indicated time points after inoculated with P6497 or PsAvh113 knockout mutants. Asterisks indicate significant differences according to Student's t-test (**P < 0.01, ns, significant difference). (**g**) The expression levels of *AtCAT1* in *PsAvh113* transgenic *Arabidopsis* plants were determined by qRT-PCR. *AtActin* gene was used as an internal control. *GmEF1a* gene was used as an internal control in (f). Data in (f) and (g) represent mean ± standard error (SE). Different letters indicate statistically significant differences (P < 0.01; Duncan's multiple range test). The experiment was performed in triplicate with similar results.

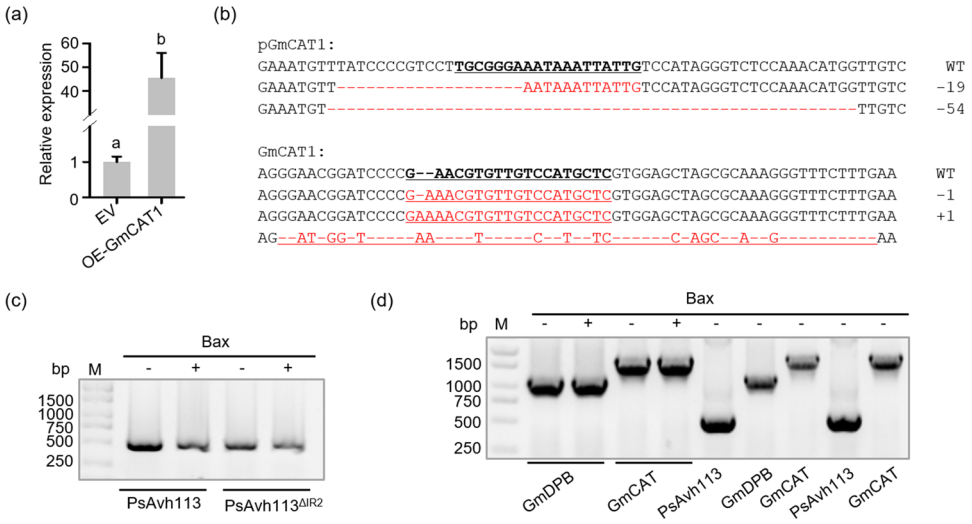

Figure S9 Analysis of expression and editing sequence in *GmCAT1*-overexpressed and *pGmCAT1 or GmCAT1*-edited soybean hairy roots.

(**a**) The transcription level of *GmCAT1* in *GmCAT1*-overexpressed soybean hairy roots by qRT-PCR. (**b**) Sanger sequencing in *pGmCAT1*-edited and *GmCAT1*-edited soybean hairy roots. (**c**)–(d) The transcriptional levels of *PsAvh113*, *GmCAT* and *GmDPB* in *N. benthamiana* were determined by RT-PCR. The experiment was performed in twice with similar results.